Journal of Mechanical Engineering and Sciences
ISSN (Print): 2289-4659; e-ISSN: 2231-8380
Volume 13, Issue 3, pp. 5242-5258, September 2019

DOI: https://doi.org/10.15282/jmes.13.3.2019.03.0429

Performance enhancement of normal contact ratio gearing system through correction factor

R. Ravivarman[1*], K. Palaniradja[2], R. Prabhu Sekar[3]

[1] Department of Mechanical Engineering, Easwari Engineering College, Chennai, India
[2] Department of Mechanical Engineering, Pondicherry Engineering College, India
[3]Mechanical Engineering Department, Motilal Nehru National Institute of Technology, Allahabad, Uttar Pradesh, India
*Corresponding author: varman92@gmail.com, palaniradja72@pec.edu, prabhusekar.r@gmail.com

ABSTRACT

Higher transmission ratio drives system will have uneven stresses in the root region of the pinion and wheel. To enrich this agility of uneven stresses in normal-contact ratio (NCR) gearing system, an enhanced system is desirable to be industrialized. To attain this objective, it is proposed to put on the idea of modifying the correction factor in such a manner that the bending strength of the gearing system is improved. In this work, the correction factor is modified in such a way that the stress in the root region is equalized between the pinion and wheel. This equalization of stresses is carried out by providing a correction factor in three circumstances: in pinion; wheel and both the pinion and the wheel. Henceforth performances of this S_+, S_0 and S_- drives are evaluated in finite element analysis (FEA) and compared for balanced root stresses in parallel shaft spur gearing systems. It is seen that the outcomes gained from the modified drive have enhanced performance than the standard drive.

Keywords: Correction factor; finite element analysis; performance; root stress; spur gear drive

INTRODUCTION

In general, the strength in gears is majorly influenced by the geometry of the tooth profile. The two major concerns under which the gear teeth fail is due to failure in bending and contact pressure which leads to miscarriages on the surface of the tooth profile. The modification of addendum was studied by D. Gunay et.al [1] in tooth profile using finite element analysis and predicted the variation of the tooth thickness in addendum with the radius of the fillet for the corrected gear drives. Chernets et al. [2-3] derived a model for the valuation of the material loss in the surface of the tooth based on its toughness and hardness with the effect of profile correction. Shuting Li [4-5] extended discussion on the modifications of the gear tooth with its error in machining and assembly on the load-carrying capacity of the drive added advantage to corrected gears. The displayed after effects of investigations on the impact of correction of the teeth on the contact and root stress were not discussed. The advancement of performance properties in the involute gearing with the inclusion of correction factor acquires prominence when compared along uncorrected gears.

At the present scenario, the tooth profile with involute shapes finds intense applications on the modification of addendum and also they attain their valuable properties when paralleled to uncorrected tooth profiles. The application of correction factor will add advantages like manufacturing gears with less number of teeth by eliminating interferences and under cutting during meshing, a suitable alternate for the manufactures who is in need to vary the centre distance.

It turns out to be essential to predict in the way, the loading actually varies on the gear tooth which depends on deflection, sliding, tooth wear among the adjacent tooth pairs. Prabhu Sekar and Muthuveerappan [6] predicted the prominence of load sharing [7] ratio through balanced root stress of non-standard NCR spur gear drive and explained the significance of load share on the stresses. Thus the reduction of root stresses gets noticed [8-9] with its eminence and improvement in the design stage itself. The widespread of deformation in the gear pair teeth profile comprises of two: one by the Hertz contact [10] and the other by the tooth bending in the root region. Furthermore, the transmission systems drives with less deflection will tend to decrease the root stress in turn reducing the load share in the contacting teeth which will have a reduced effect on the contact stress. This effect will also reduce the wear depth in the teeth profile. Tunalioglu [11-12] discussed about the tooth wear in the internally developed drives. With the extension of numerical simulation which enables the designers to anticipate the stresses precisely as though in the physical model utilizing the Finite Element Methods (FEM). Thus, contact analysis through FEM attains its fame in estimating the contact stresses on the tooth profile which is a distinctive valuation method applied to transmissions systems [13-14]. The transmission drive will normally require a non-conformal contact together with the sliding and rolling mechanisms in a gear tooth. Thus, the major factors that constitute for mechanical efficiency are sliding power loss and rolling power loss components. Mechanical efficiency of the parallel-axis gear pairs was predicted by Xu et.al [15] in its model which included both the above mentioned components in their study. The model of frictional sliding coefficient was used by Wang et al. [16], Mihailidis and E. Athanasopoulos [17] in predicting the losses in gear drives. This methodology is used in this work to predict the losses in the gear drive along the path of contact.

The available literature on the correction factor of the tooth profile is incomprehensive which not discuss about the balanced bending strength. Main objective of this work is to minimize the stresses in bending by balancing it between the drives and reducing the contact stress among the pairs which are engaged during meshing. Thereby, predicting the complete performance parameters such as sliding distance, coefficient of friction, film thickness, wear depth, power loss and finally the mechanical efficiency of the modified gear drives.

CRITICAL LOADING POINTS IN NORMAL CONTACT RATIO TRANSMISSION SYSTEM

For the transmission system, the province of the tooth profile taking the critical load points is determined. The prominent phase of the problem is generating the involute and trochoid tooth profile for the teeth. The profile of the tooth is spawned in Ansys Parametric Design language (APDL). The standard gear drive (x_p=0, x_g=0) and the corrected gear drive (x_p=+0.1, x_p=-0.1) is plotted and the variation in the tooth profile is shown in Figure 1. From

the line diagram, it is observed that the critical tooth thickness in the root region is increased for a positive drive (x_p=+0.1) whereas it is decreased in the negative drive (x_p=-0.1) which will play a vital role in balancing the root stress.

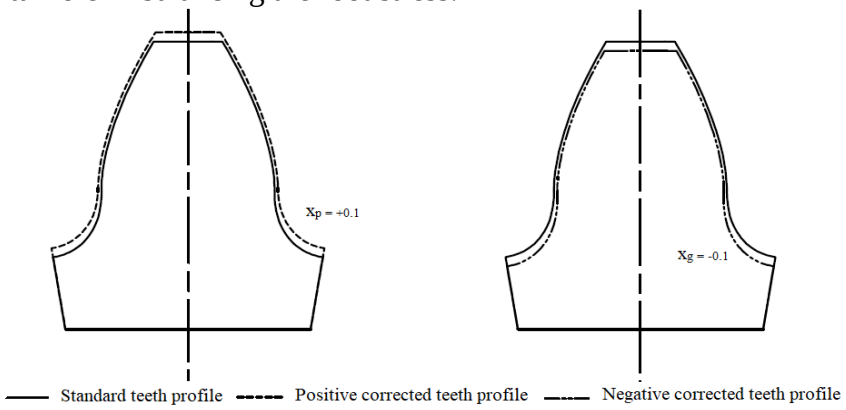

Figure 1. Teeth profile layout comparison between the standard and corrected

For the transmission system considered, the mechanics of tooth engagement during the full rotation of teeth is revealed in Figure 2. The sets of teeth which comes in contact will initiate the engagement at the point-A which is the highest point of tooth contact (HPTC), during this engagement two sets of teeth come in contact by sharing the total load in two positions at point-A in one tooth and at point-B, highest point of single tooth contact (HPSTC) in the adjacent leaving teeth which is a double pair contact-AB. The next trailing pair is a single pair contact-BC where C is the lowest point of single tooth contact (LPSTC). And the final trailing pair-CD which will be again converted into a double pair region since the next trailing tooth will come to contact during the transmission. In the complete contact path of teeth, only the adjacent teeth on both side comes in contact with the teeth considered which allows to develop a three teeth model in FEM for contact analysis. This will in turn reduce the computational time when compared to a full model. Prabhu Sekar [6, 13] made an effort to consider the critical contact points of standard spur gear drive design model in his study. As suggested, by the authors the balancing of root stress is carried in the present work through modification in correction factor. Radial distances proposed [6] to compute the critical contact points for corrected gears are stated by the Equations (1) to (4).

$$r_{HPTC} = r_{awp} \tag{1}$$

$$r_{HPSTC} = \sqrt{\left(\sqrt{r_{awp}^2 - r_{bp}^2} + p_{bw} - AD\right)^2 + r_{bp}^2} \tag{2}$$

$$r_{LPSTC} = \sqrt{\left(\sqrt{r_{awp}^2 - r_{bp}^2} - p_{bw}\right)^2 + r_{bp}^2} \tag{3}$$

$$r_{LPTC} = \sqrt{\left(\sqrt{r_{awp}^2 - r_{bp}^2} - AD\right)^2 + r_{bp}^2} \tag{4}$$

$$AD = \sqrt{r_{awp}^2 - r_{bp}^2} + \sqrt{r_{awg}^2 - r_{bg}^2} - a_w \sin \alpha_w \tag{5}$$

where, AD Line of action of the contact
a_o Centre distance
p_{bw} Base pitch in mm
r_{awp} Radius of addendum working circle for pinion
r_{HPSTC} Radii at HPSTC point for pinion
r_{HPTC} Radii at HPTC point for pinion
r_{LPTC} Radii at LPTC point for pinion
r_{LPSTC} Radii at LPSTC point for pinion
r_{bp} Base circle radius for pinion

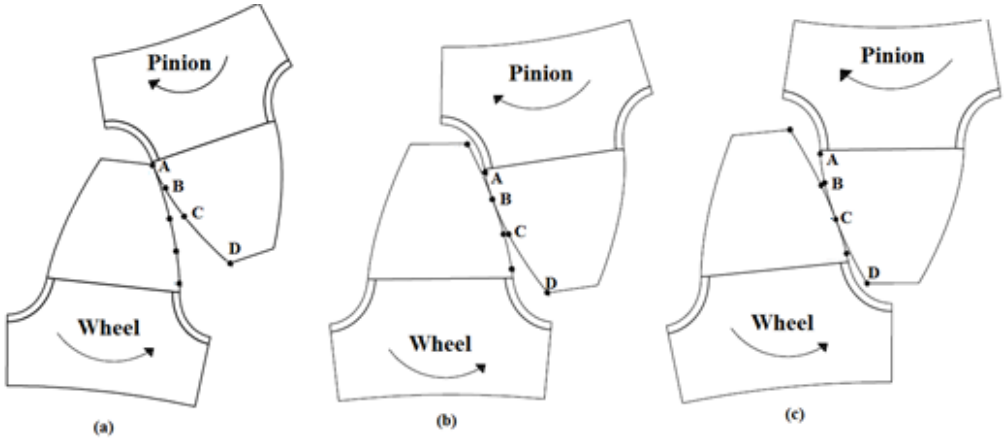

Figure 2. Mechanics of critical contact points in normal contact ratio gear system

MULTI POINT ANALYSIS NUMERICAL MODEL USED FOR STUDYING THE TRANSMISSION SYSTEM

In Figure 3 a bi-dimensional FE Model using quadrilateral PLANE82 element is established to calculate the load share, contact stress and root stress. As suggested to reduce the computational timing, only three teeth pair is established since remaining teeth has zero effect on the calculation of mesh stiffness. The geometry of the spur gear drive taken for FEA modelling is given in Table. 1. For the boundary conditions, the inner node of the driven gear (wheel) is fully restrained and the driving gear (pinion) is only allowed to rotate around the gear axis. According to the direction of rotation, an equivalent torque is applied to the nodes of the driving gear (pinion) in the clockwise direction. The constraints and the load needed for the analysis is applied to the model as mentioned (See Figure3). Poisson's ratio (ν) is taken as 0.3 and a plane stress condition is taken in this work since the face width is assumed to be uniform along the spur gear drive system. For elasticity concerned it is taken as linear throughout the model. In this FE Model, the load share model is taken for the study which considers both the root and contact stress. For contact analysis, the target element (TARGE169) and contact element (CONTA172) is defined with an automatic contact adjustment of close gap between the surfaces. The contact algorithm used to compute is Augmented Lagrange.

Table 1. Geometrical parameters of the spur gear drive

Parameter	Symbol	Value
Tooth number	z_p	20
Pressure angle (degree)	α_o	20^0
Transmission ratio	i	1.5
Module (mm)	m	1
Normal Speed (rpm)	N_p	150
Modulus of rigidity (GPa)	E	210
Rim thickness (mm)	r_t	5
Addendum height (mm)	h_a	1
Normal load (N)	F_N	10

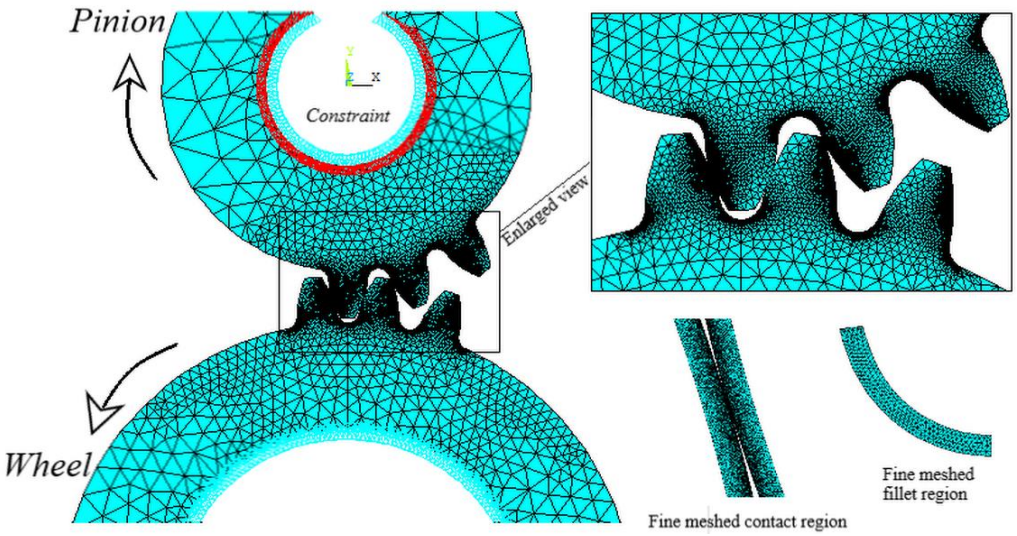

Figure 3. FEM of the transmission drive

PREDICTION OF THE PERFORMANCE FACTORS IN ADDENDUM MODIFIED EXTERNAL TRANSMISSION GEAR SYSTEM

A satisfactory bending strength is achieved by setting the tooth root stress balance between the pinion and wheel as constraints through profile modification technique. The efficiency of the modified drive will be discussed using the results obtained by the application of the finite element method. In general, the mechanical efficiency (η) of the gearing system is conveyed by,

$$\eta = \left(\frac{P_{input} - P_{loss}}{P_{input}}\right) X100 \quad (6)$$

The power input is predicted from the applied torque and the rotational speed which is given as input to the drive. In the case of the power loss, it will depend upon numerous losses that

occur in the drive during transmission. The gear teeth which are interacting against one another will undergo both sliding and rolling actions which will create mesh losses in the drive. Thus, the mesh loss of the gear drive will account for both the rolling and sliding component of the drive system.

Total mesh power loss for any instantaneous teeth pair is taken as,

$$(P_{loss})_i = (P_S)_i + (P_R)_i \tag{7}$$

POWER LOSS DUE TO SLIDING COMPONENT

The sliding power loss mainly arises due to the development of frictional forces among the interacting gear teeth profiles. This sliding power loss is the direct measure of the frictional sliding force (F_S) and the sliding velocity (v_S) which is given as,

$$(P_S)_i = (F_S)_i (v_S)_i \tag{8}$$

Where,

$$\text{Sliding force}(F_S) = \mu_i F_i \tag{9}$$

$$\text{Sliding velocity } (v_S)_i = \left|(v_p)_i - (v_g)_i\right| \tag{10}$$

The magnitude of the sliding force will be the measure of the load shared among the teeth during contact which is obtained through FEM and the coefficient of friction (μ) between the contacting surfaces.

To determine the coefficient of friction (μ) the model suggested by Xu [15] was considered and given as,

$$\mu_i = e^{f(SR_i,(\sigma_H)_i,\gamma_{0,s})} (\sigma_H)_i^{c_2} |SR|_i^{c_3} (v_e)_i^{c_6} \gamma_0^{c_7} R_i^{c_8} \tag{11}$$

Where function is taken as,

$$f(SR_i, (\sigma_H)_i, \gamma_0, s) = c_1 + c_4 |SR|_i (\sigma_H)_i \log \gamma_0 + c_5 e^{-|SR_i| \log \gamma_0 (\sigma_H)_i} + c_9 e^s \tag{12}$$

Here the values of c_i= -8.92, 1.03, 1.04, -0.35, 2.81, -0.10, 0.75, -0.39 and 0.62 for i = 1 to 9 with absolute viscosity γ_o is 0.0065 Pas. The RMS composite roughness factor (s) is taken as 0.1μm with an inlet temperature of 373.15 K. The temperature viscosity coefficient δ = 0.1176 (1/K) and the pressure viscosity coefficient ρ =1.2773x 10^{-8}(1/Pa) is taken respectively. [15]

The Slide to roll ratio (SR) is obtained from the relation,

$$(SR)_i = \frac{(v_S)_i}{(v_e)_i} \tag{13}$$

Where the entraining velocity (v_e) is given as [18]

$$(v_e)_i = \frac{1}{2}\left|(v_p)_i + (v_g)_i\right| \tag{14}$$

In the above eqn. (14), v_p are v_g are the peripheral velocity which is multiple of the angular velocity and the radius of curvature at any instantaneous contact point.

POWER LOSS DUE TO ROLLING COMPONENT

The rolling component power loss is primarily initiated by the development of the hydro dynamic contact pressure between the gear tooth surfaces which creates an elastohydrodynamic (EHL) film among the mating surfaces. This film thickness will tend to absorb power that is created by the relative motion of the mating teeth pair. The instantaneous rolling power loss $(P_R)_i$ in W is calculated by the model recommended by Anderson and Loewenthal [19],

$$\text{Rolling Power Loss } (P_R)_i = (F_R)_i (v_R)_i \tag{15}$$

Where,

$$\text{Rolling Force } (F_R)_i = 9 * 10^7 \phi_t \, (\varphi_L)_i b \tag{16}$$

$$\text{Rolling velocity } (v_R)_i = \left|(v_p)_i + (v_g)_i\right| \tag{17}$$

Where, ϕ_t-Thermal reduction factor

To calculate the EHL film thickness (φ_L) during contact the Hamrock and Dowson [20] model is used which is given as,

$$(\varphi_L)_i = 2.69 \, U_i^{0.67} G^{0.53} L_i^{-0.067} (1 - 0.61e^{-0.73K}) R_i \tag{18}$$

Where,

$$\text{Speed parameter, } U_i = \frac{(v_e)_i \gamma_0}{E' R_i} \tag{19}$$

$$\text{Material parameter, } G = E'\rho \tag{20}$$

$$\text{Load parameter, } L_i = \frac{F_i}{E' R_i^2} \tag{21}$$

In which the, Equivalent modulus of rigidity (E') and Equivalent radius of curvature (R_i) at any instantaneous contact are evaluated from the respective wheel and pinion. The ellipticity factor (K) is considered as 12 for contact between the gear pair [19]. In Equations (16) the thermal reduction factor (ϕ_t) is taken from Cheng [21] model of prediction of film thickness in EHL contacts.

WEAR DEPTH PREDICTION ALONG THE TOOTH PROFILE

Generalized equation for predicting wear depth (h) is considered from the Anderson wear model [18] as

$$h = \int_0^S K_h \, \sigma_H ds \tag{22}$$

The generalized equation considered by Anderson and Erikson [22] to develop the contact procedure for computing the accumulated wear depth is specified as,

$$h_{i,n} = h_{i,(n-1)} + K_h (\sigma_H)_i \left(s_p\right)_i \tag{23}$$

where,

K_h=5x10^{-16} m^2/N, Dimensionless wear co-efficient [18].

Sliding distance at any instantaneous contact points is given by,

$$(s_p)_i = 2a_i\left(\frac{(v_p)_i - (v_g)_i}{(v_p)_i}\right) \tag{24}$$

In which, semi contact width (a_i),

$$a_i = \sqrt{\frac{4F_i}{\pi b}\frac{\frac{(1-\nu_p^2)}{E_p}+\frac{(1-\nu_g^2)}{E_g}}{\frac{1}{(R_p)_i}+\frac{1}{(R_g)_i}}} \tag{25}$$

Where,

ν - Poission's ratio.

E - Modulus of rigidity in GPa.

From the assessed wear depth (Equations (23)), the worn out amount of material from the surface of teeth during each mesh cycle is estimated and updated in the profile. The outline of the teeth profile which gets worn out teeth is exposed in Figure 4. After number of mesh cycles the co-ordinates is specified as

$$x_i' = x_i - h_i\cos\theta_i' \tag{26}$$

$$y_i' = y_i - h_i\sin\theta_i' \tag{27}$$

where, The initial involute profile is taken as,

$$x_i = R_i\cos\Theta_i \tag{28}$$

$$y_i = R_i\sin\Theta_i \tag{29}$$

Where, θ_i' -Tooth thickness at contact in degree

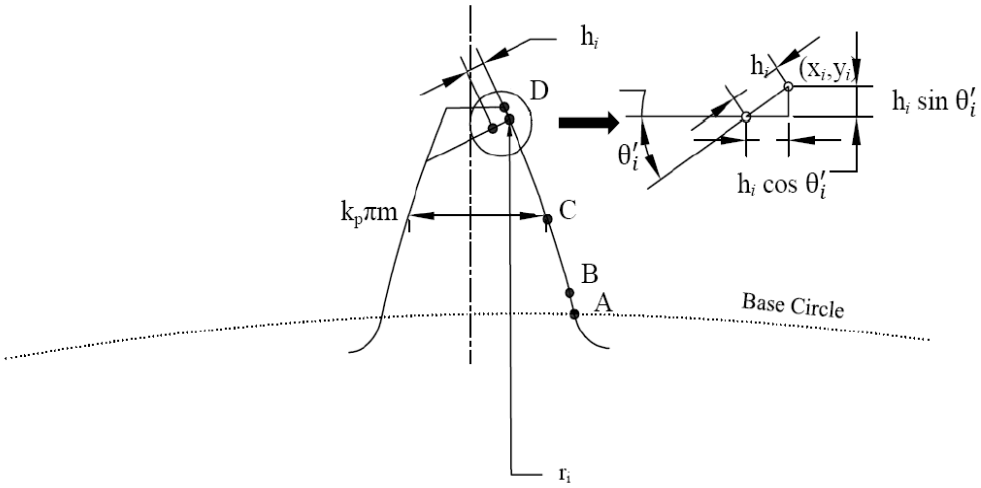

Figure 4. Layout of the tooth profile

STUDY AND VALIDATION

In this section, the simulation parameters considered for drives are as trails: $z_p = 20$, $\alpha_o = 20^o$, i = 1.5, m = 1 mm, $F_N = 10$ N, $h_a = 1$ mm and $h_f = 1.25$ mm. The load share ratio (F_i) for the gear pairs is obtained for drive combinations of: Standard, S_+, S_-, and S_0 drives, as shown in Figure 5. In the Figure 5(a), HPTC-A denotes the beginning of engagement point and LPTC-

D denotes the ending of engagement point of the drives for one mesh cycle. In the corrected gears, Figure 5.(a) whether it is a positive or negative correction the load share decreases in the first pair of double tooth contact-AB and it increases the same amount share in the second pair of double tooth contact-CD whereas the single tooth contact-BC takes the full normal load (F_N) which agrees with the same trend of standard gear drives [23].

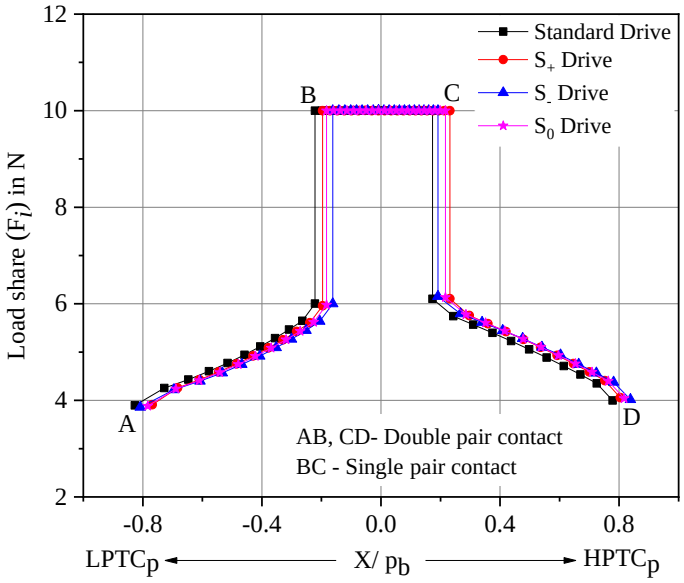

(a) Variation of load share ratio (F_i) along line of action

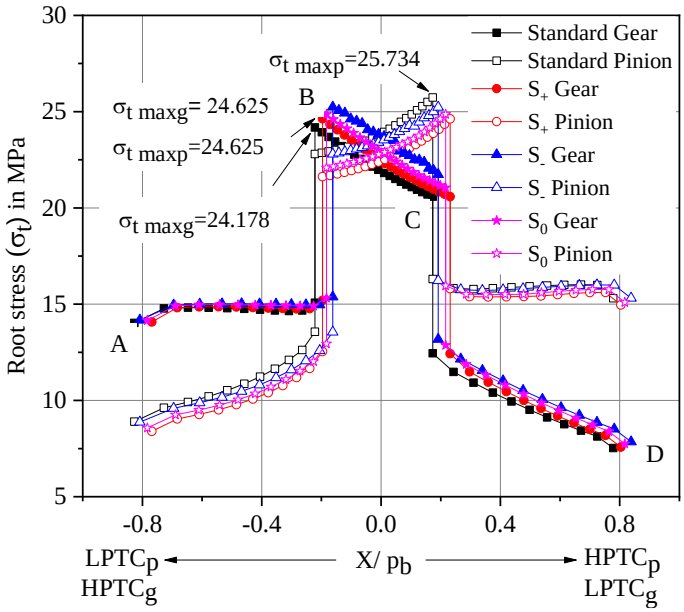

(b) Variation of root stress (σ_t) along line of action

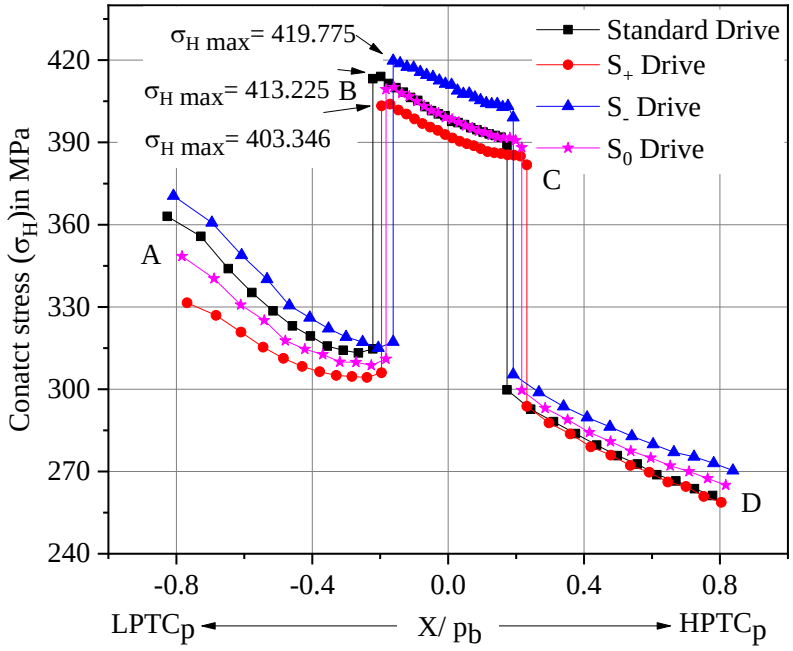

(c) Variation of contact stress (σ_H) along line of action

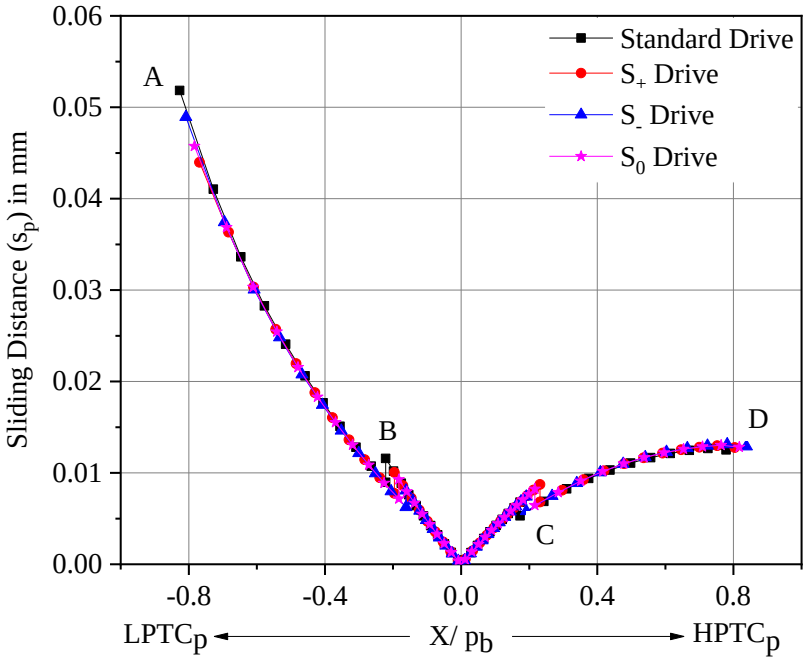

(d) Variation of sliding distance (S_p) along line of action

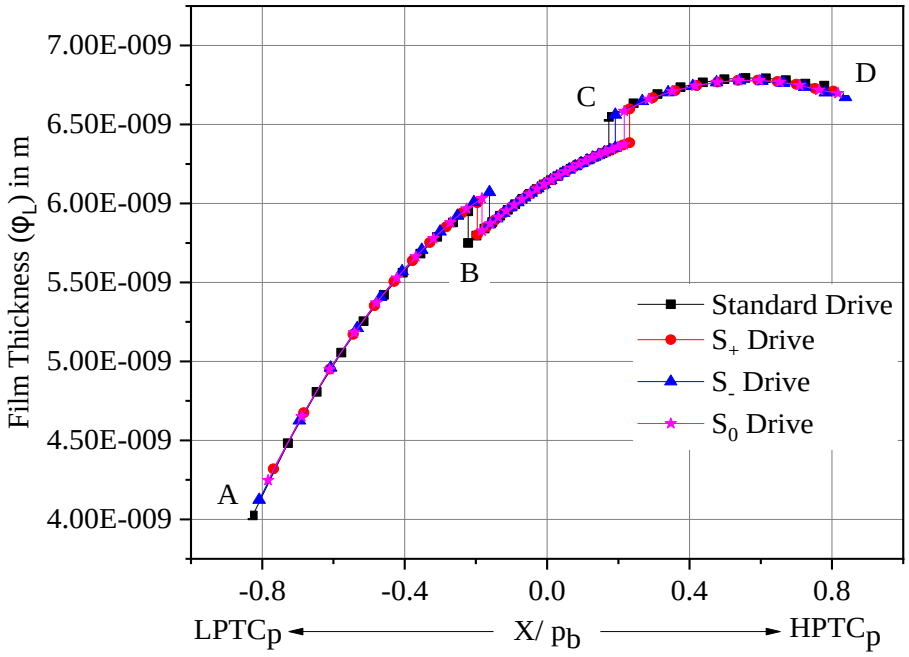

(e) Variation of film thickness (h_L) along line of action

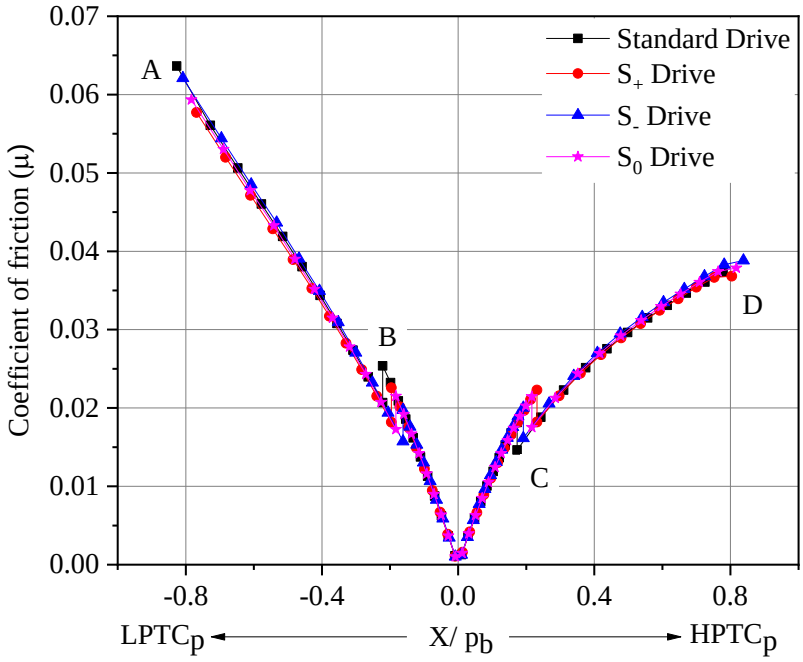

(f) Variation of coefficient of friction (μ) along line of action

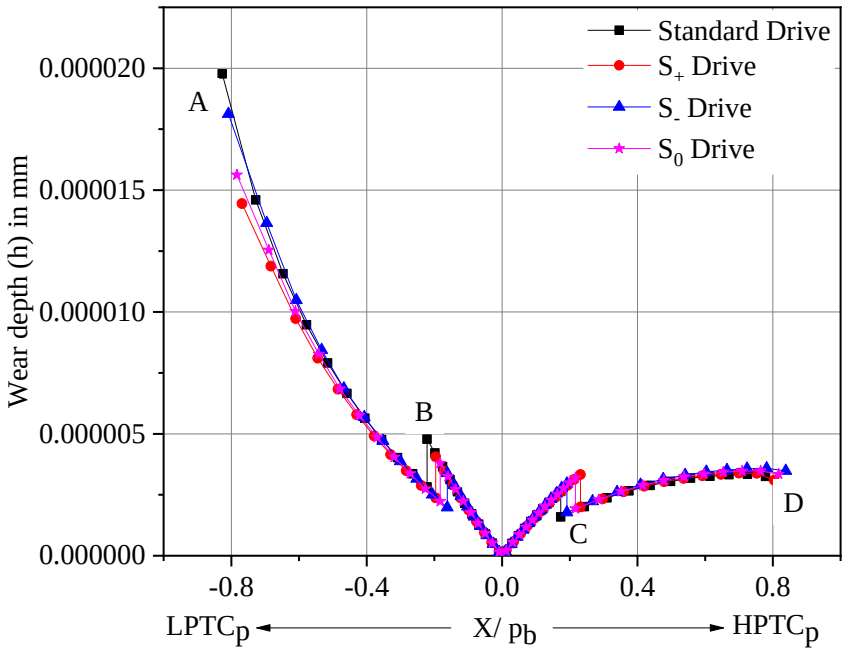

(g) Variation of wear depth (h) along line of action

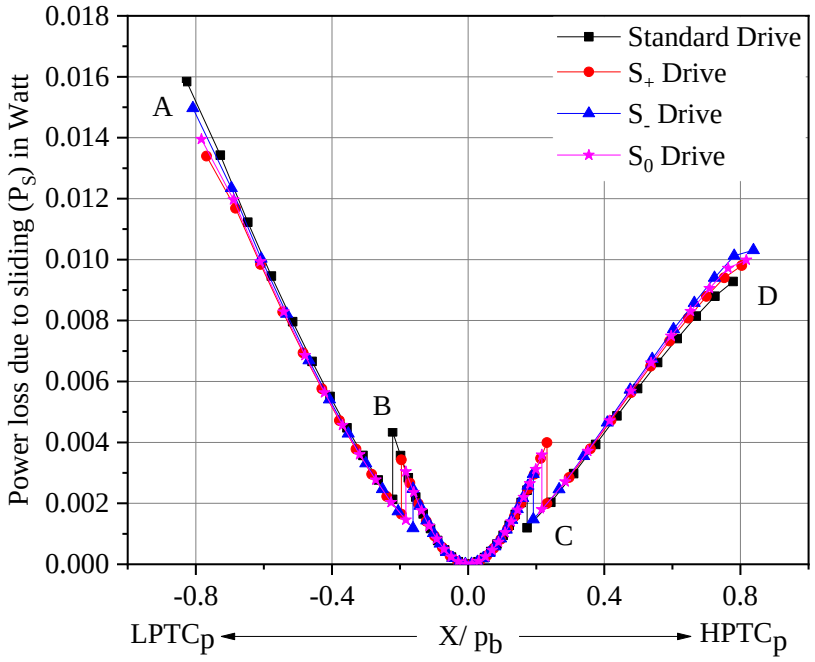

(h) Variation of sliding power loss (P_S) along line of action

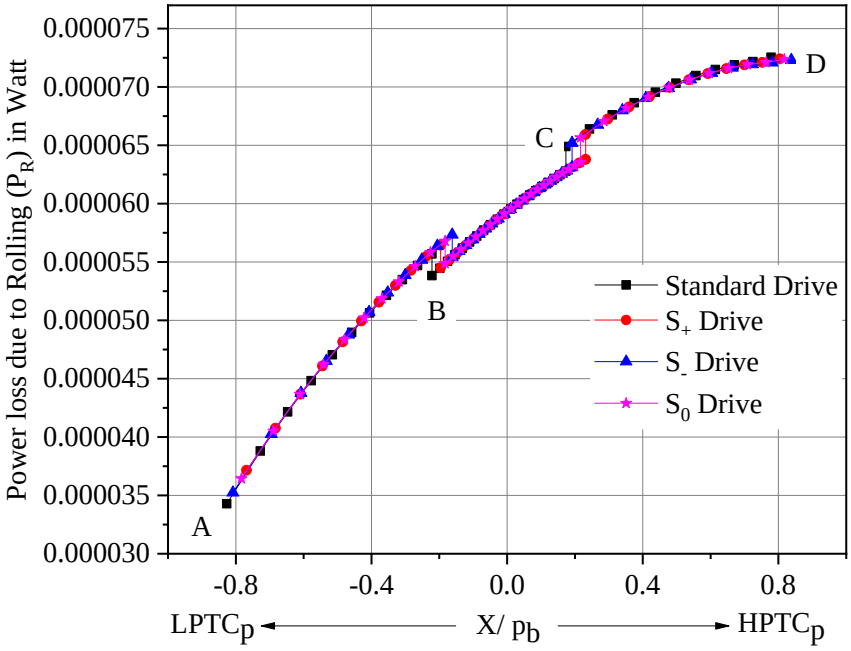

(i) Variation of rolling power loss (P_R) along line of action

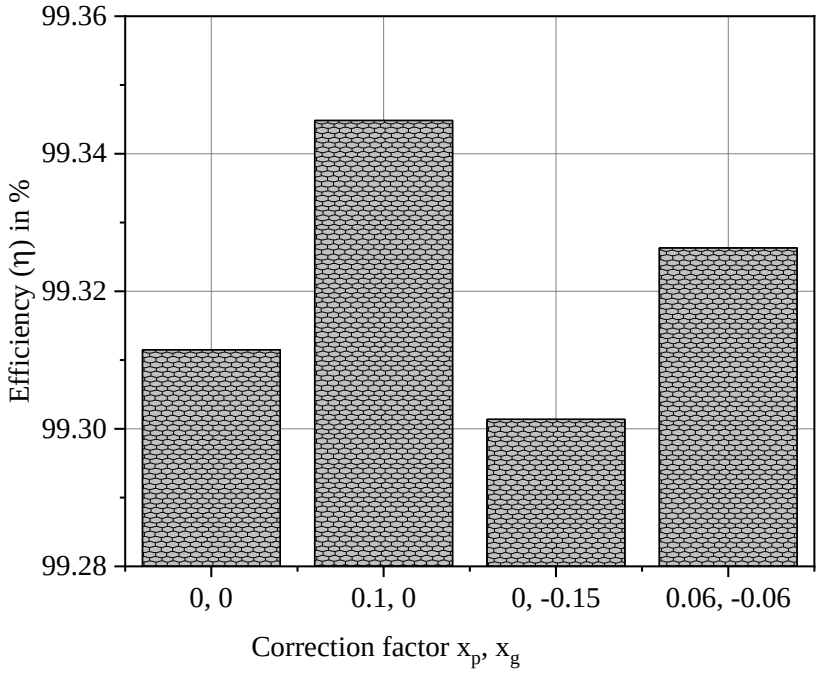

(j) Variation of efficiency (η) with correction factor.

Figure 5. Assessment of gear performance with different combination of correction factor

The stresses obtained corresponding to the drives is listed in Table 2. which shows the difference among the stresses between wheel and pinion for standard and corrected drives. This uneven stresses is balanced by applying correction factor which improves the bending strength of the drive. It is worth noting that the root stress for positive corrected drives of the pinion reduces to $(\sigma_t)_{max\ p}$ = 24.6225 MPa (Figure 5(b)) from 25.7341 MPa of standard drives thereby balancing the bending strength among drives. In the positive corrected drives, the critical tooth thickness increases in the pinion root region and the same amount of tooth thickness decreases at the gear root region. Because of this reason, the root stress decreases in the pinion and it increases in the gear in the positive addendum modified gear drives. This effective range of improvement in the bending strength gets attention in this work.

Table 2. FEA results compared between combinational drives

Drives	Correction Factor		Root Stress		Contact Stress
	x_p	x_g	$(\sigma_t)_{max\ p}$ MPa	$(\sigma_t)_{max\ g}$ MPa	$(\sigma_H)_{max}$ MPa
Standard Drive	0	0	25.7341	24.1785	413.2255
S_+ Drive	0.1	0	24.6255	24.6275	403.3468
S_- Drive	0	-0.15	25.2355	25.2369	419.7752
S_0 Drive	0.06	-0.06	24.8621	24.8635	409.3513

The actual range of contact stress is prolonged by the variation in the range-length as shown in Figure 5(c). The contact stress is maximum at point-B LPSTC in the single-tooth engagement of full load (Table 2 and Figure 5(c), [23]). It is noticed that S_- drive have larger amount of stress at B than that of the other drives which is influenced by the decrease in the radius of curvature. It is also observed that the maximum contact stress $(\sigma_H)_{max}$ is achieved minimum for the positive corrected drives compared to standard and other combinational drives because of increased radius of curvature. These variations are observed for both the pinion and wheel of the transmission system due to change in the radius of curvature along the line of action of the teeth profile. The sliding distance decreases (Figure 5(d)) in the S_+ drives in comparison with other drives which are mainly influenced by the corresponding decrease in the sliding velocity ratio (Equations (24)). It is also inferred that the sliding distance decreases at LPTC (point A) in S_+ drive which is mainly due to the shifting of LPTC point towards the pitch point. Due to pure rolling action at the pitch point, the sliding motion is zero. From the Figs. 5(e and f) it is observed that the coefficient of friction (Equations (11)) is achieved minimum for S_+ drives due to reduced slide to roll ratio whereas the EHL film thickness is witnessed to be increased (Equations (18)) for the same drive due to the corresponding rise in the equivalent radius of curvature when compared with other drives. It is predicted from the Equations (23) that the wearing of teeth is less for a balanced S_+ drives (Figure 5(g)) when compared to the other balanced case drives and the standard one. This is mainly due to the reduced sliding distance and contact stresses along the tooth profile of the engaging teeth surfaces. Fig 5(h) shows the trend of sliding power loss, which is seen to be reduced in the AB region for S_+ drives that is majorly influenced by the reduction of load share in the same region and also the combinational reduction of coefficient of friction and

contact stress in region-AB. The rolling power loss deviation is negligible (Figure 5(i)) and similar to the EHL film thickness since it is majorly influenced by the variation of EHL film thickness itself. It is evident from the power loss trend that S_+ drives have minimal losses which is directly seen in the efficiency plot (Figure 5(j)). This minimal loss ultimately increases the efficiency of the corrected drive making S_+ drive has the most efficient one in terms of balanced bending strength.

CONCLUSIONS

1. For the standard and corrected gears, appropriate addendum modifications are made and recommended to attain an improved and balanced strength while design a spur gear pair.
2. A uniform decline in the amount of stress (both root and contact), sliding distance, and friction coefficient was evaluated with enhanced wear resistance and efficiency on the operational surfaces of the profile teeth as an outcome of positive correction (S_+) factor which makes it the better one in terms of overall performance for equalized bending strength.
3. It is observed that the negative corrected (S_-) drive is having less efficiency and contact strength when compared with standard and other corrected drives. Hence it is not preferable to provide negative correction to drives while balancing the stresses.

ACKNOWLEDGMENTS

This research was supported by INSPIRE Fellowship scheme, Department of Science and Technology (DST) Government of India, for the corresponding author by providing financial assistance.

REFERENCES

[1] Gunay D, Ozer H, Aydemir L. The effects of addendum modification coefficient on tooth stresses of spur gear. Mathematical & Computational Applications. 1996;1(1): 36-43.

[2] Chernets MV, Yarema RY, Chernets Y. M. A method for the evaluation of the influence of correction and wear of the teeth of a cylindrical gear on its durability and strength. Part 1. Service life and wear. Material Science. 2012;3:289–300.

[3] Chernets MV, Yarema RY. On the problem of the evaluation of the influence of correction of teeth of a cylindrical involute helical gear on its contact strength. Probl. Tribol. 2011;4:26–32.

[4] Shuting L. Effects of machining errors, assembly errors and tooth modifications on load-carrying capacity, load-sharing rate and transmission error of a pair of spur gear. Mechanism and Machine Theory. 2007;42:698–726.

[5] Shuting L. Effects of misalignment error, tooth modifications and transmitted torque on tooth engagements of a pair of spur gears. Mechanism and Machine Theory. 2015;83:125-136.

[6] Prabhu SR, Muthuveerappan G. A Balanced Maximum Root stresses on Normal Contact Ratio Spur Gears to Improve the Load Carrying Capacity through Non-Standard Gears. Mechanics based design of structure and machines, Taylor and Francis. 2015;43:150-163.

[7] Pedrero JI, Pleguezuelos M, Artés M, Antona JA. Load distribution model along the line of contact for involute external gears. Mechanism and Machine Theory. 2010;45(5) :780–794.

[8] Kapelevich AL, Shekhtman YV. Direct gear design: bending stress minimization. Gear Technology. 2003;20(5):44–47.

[9] Pedersen NL. Reducing bending stress in external spur gears by redesign of the standard cutting tool. Structural and Multidisciplinary Optimization. 2009;38(3):215–227.

[10] Ravivarman R, Palaniradja K, Prabhu SR. Evolution of balanced root stress and tribological properties in high contact ratio spur gear drive. Mechanism and Machine Theory. 2018;126:491–513.

[11] Tunalioglu MS. A Research of Tooth Profile Damages in Internal Gears. Gazi University Institute of Science and Technology, Ankara. 2011:1-5.

[12] Tunalioglu MS, Tuc B. Theoretical and experimental investigation of wear in internal gears. Wear. 2014;309:208-215.

[13] Prabhu SR, Sathishkumar R. Enhancement of Wear Resistance on Normal Contact Ratio Spur Gear Pairs through Non-Standard Gears. Wear. 2017;380-381:228-239.

[14] Schaffner T, Allmaier H, Girstmair J, Reich FM, Tangasawi O. Investigating the efficiency of automotive manual gearboxes by experiment and simulation. Proceedings of the Institution of Mechanical Engineers Part K-Journal of Multi-Body Dynamics. 2014;228(4):341–354.

[15] Xu H, Kahraman A, Anderson N, Maddock, D. Prediction of Mechanical Efficiency of Parallel-axis Gear Pairs. ASME, Journal of Mechanical Design. 2007;129:58– 68.

[16] Wang C, Cui HY, Zhang QP, Wang WM. An approach of calculation on sliding friction power losses in involute helical gears with modification. Proceedings of the Institution of Mechanical Engineers, Part C: Journal of Mechanical Engineering Science. 2016;230(9):1521–1531.

[17] Mihailidis A, Athanasopoulos E. EHL film thickness and load dependent power loss of cycloid reducers. Proceedings of the Institution of Mechanical Engineers, Part C: Journal of Mechanical Engineering Science. 2016;230(7-8):1303–1317.

[18] Flodin A, Andersson S. Simulation of mild wear in spur gears. Wear. 1997;207:16–23.

[19] Anderson NE, Loewenthal. Part and Full Load Spur Gear Efficiency. NASATP-1622, AVRADCOM. 1979.

[20] Hamrock BJ, Dowson O. Isothermal Elastohydrodynamic Lubrication of Point Contacts, Fully Flooded Results. Journal of Lubrication Technology. 1977;99:264-276.

[21] Cheng, HS. Prediction of film thickness and sliding frictional coefficient in elastohydrodynamic contacts. In: Design engineering technology conference, American Society of Mechanical Engineers, Evanston, USA, September. 1974:286–293.

[22] Andersson S, Eriksson B. Prediction of the sliding wear of spur gears. Proceedings of NORDTRIB. 1990;90.
[23] Thirumurugan R, Muthuveerappan G. Critical loading points for maximum fillet and contact stresses in normal and high contact ratio spur gears based on load sharing ratio. Mechanics Based Design of Structures and Machines. 2011;1:118–141.